Journal of Applied Engineering and Technological Science
Vol 6(2) 2025: 1297-1311

DESIGN AND IMPLEMENTATION OF HMI FOR MONITORING THE IMBALANCE OF CURRENT AND VOLTAGE BASED ON CALCULATION OF MAXIMUM DEVIATION MEAN VALUE METHOD

Toto Tohir[1], Supriyanto[2], Sofyan Muhammad Ilman[3*], Febi Ariefka Septian Putra[4], Raynda Bayu Sri Agustia[5], Hadrian Anwar[6], Fikhi Akmal[7]
Department of Electrical Engineering, Politeknik Negeri Bandung, Bandung Barat, Indonesia[1,2,3,4,5,6,7]
sofyan.muhammad@polban.ac.id[3]

Received: 08 October 2024, Revised: 10 March 2025, Accepted: 18 March 2025
**Corresponding Author*

ABSTRACT
Voltage and current (V-I) imbalance in a three-phase power system can cause decreased efficiency, increased power losses, equipment heating, induction machine faults, and neutral currents. The main causes of this problem are uneven load distribution, phase failure, or network disturbances. Therefore, monitoring imbalance is critical to determine the right corrective steps. This study aims to design and implement a Human-Machine Interface (HMI) as a tool to monitor voltage and current imbalance using the Calculation Maximum Deviation Mean Value (CMDMV) method. This method calculates the maximum deviation of V-I from each phase to obtain an accurate imbalance value. Current and voltage sensors are used to collect real-time data, which are then processed using CMDMV in the HMI software. The results are displayed in the form of graphs, status indicators, and percentage figures, then compared with a power quality analyzer for accuracy validation. The results show that this HMI system can display V-I imbalance in real-time with a reading error rate when the imbalance condition is below 5%, and when it detects an imbalance in V-I, the indicator turns yellow (WARNING). With the creation of this device, it can help identify V-I imbalances in each phase.
Keywords: *Imbalance, HMI, CMDMV, V-I.*

1. Introduction

The problem of voltage imbalance in a three-phase system is one of the power quality problems that often occurs in electric power systems, both in transmission and distribution networks. This problem arises due to uneven distribution of loads in three phases or a mismatch in the phase angle, which should be 120° between phases with other phases. If not identified carefully, voltage imbalance can reduce the efficiency of electrical equipment, shorten the life of induction motors, and increase power losses in the electrical system (Silva & Ferreira Filho, 2022). Research shows that imbalance can interfere with the estimation of phase synchronization, frequency, and the rate of change of frequency (Rate of Change of Frequency, ROCOF) in the electric power network, thus affecting the control system and network automation (Castello et al., 2018). This imbalance not only increase harmonic voltage and current, but also contribute to a decrease in the power factor and increase power losses in the electricity distribution system. In addition, studies have shown that an imbalanced system can cause power fluctuations that contribute to operational disruptions and decreased efficiency of electrical equipment (Czarecki, 1995). On the other hand, load imbalance in a three-phase four-wire inverter can significantly reduce the reliability of semiconductors used in power electronic devices. The difference in current between phases causes uneven heat distribution in semiconductor devices, thereby shortening the life of the system. In addition, the presence of harmonics in the load current exacerbates semiconductor degradation due to increased voltage and greater temperature fluctuations (Lledó-Ponsati et al., 2021). Furthermore, in a Phase-Locked Loop (PLL)-based control system, voltage and current imbalances can cause errors in phase angle and frequency estimation, which impact the accuracy of the synchronization system. The presence of harmonics and interharmonics further exacerbates the imbalance, causing errors in frequency estimation and affecting the stability of the PLL control system. Therefore, a thorough understanding of the characteristics of imbalance in the power system and its mitigation methods is very important to maintain the reliability and efficiency of the power

system, especially in facing the challenges of renewable energy integration (Feola et al., 2013). In electrical machines, devices such as induction motors are often used in various industrial applications because of their reliability, but they are very sensitive to imbalanced voltage variations. Imbalanced voltages can cause increased power losses, increased temperatures, and decreased efficiency and motor life (Kersting, 2001). Therefore, a voltage and current imbalance monitoring tool is needed to assist users in taking appropriate corrective actions based on the recommendations given. One solution that can be applied is a Human-Machine Interface (HMI)-based monitoring system that is able to monitor and analyze voltage and current imbalances in real-time. Especially in the automation sub-section that supports the field. Starting from generation, transmission, and distribution systems to electrical energy. For now, it has also begun to develop and grow in the application of intelligent electricity networks, better known as smart grids where, with this concept, electricity networks can be monitored in real-time in which several information, communication, control, and measurement technologies have been embedded to increase the reliability and security of the network system (Kulkarni et al., 2021)(Reza et al., 2020). In addition to the electricity network sector, software technology in the automation field has also grown and been applied to the industrial control sector. Meanwhile, almost all industrial control devices currently have an embedded Human Machine Interface (HMI) system. This system supports complex industrial processes and controls by monitoring and controlling all existing systems in the industry. Several HMI frameworks have been modified into mobile systems (Qasim et al., 2020).

Research on HMI and Supervisory Control and Data Acquisition (SCADA) proliferates in various sectors of electrical energy generation, electrical substations, electrical networks, industry, commercial buildings, and vehicles. Research on SCADA systems for remote monitoring and control utilizing communication protocols has been conducted. This research visualizes data processing on the HMI screen in the control center. However, with this method of visualization by technicians, maintenance, supervision, and control procedures are prone to errors. Hence, this research proposes a new technique in visualization, namely augmented reality (AR) and mixed reality (MR), which method provides a new way to display relevant data (Antonijević et al., 2018).

2. Literature Review

Research on management platforms to determine equipment status and maintenance using a SCADA-based monitoring system that applies intelligent control using fuzzy theory to classify factors that influence equipment (Gu et al., 2019). Apart from the HMI and SCADA software side, which is implemented at primary substations, another side that has been researched is regarding data security in the SCADA system, where currently electricity systems are integrated with telecommunications equipment, and information containing complete data from a sub-system but vulnerable to eavesdropping and attacks on the software side, so research on the trust-based framework method for substations on smart grid networks is designed and implemented (Boakye-Boateng et al., 2024). SCADA system and substation automation to monitor and protect devices in a port undergoing a power supply upgrade (Mnukwa & Saha, 2020). Developing a SCADA gateway to combine existing conventional systems at main substations, which has the advantage of installing the latest equipment and integration into main substations, can be done efficiently (Basuki et al., 2011). Web-based monitoring, controlling, and data acquisition systems have been applied to substations and electrical energy generation (Lahti et al., 2011)(Craig Wester, Noel Engelman, Terrence Smith, Kehinde Odetunde, Bob Anderson, 2015). A reliability analysis of the SCADA system was conducted to analyze its performance (Bruce, 1997). The monitoring system can be integrated with the new renewable energy generation system (Biswal & Bansal, 2015) dan and on the smart grid (Raman et al., 2014). The development of monitoring methods using HMI for industrial control processes using a multiagent approach to visualize devices with unconventional devices combined with natural user interaction (Skripcak et al., 2013) as the key to implementing automation 5.0, namely having a request system towards industry 5.0 (Vlacic et al., 2024)(Šverko & Grbac, 2024). In addition to these systems dominating in supporting the monitoring of complex industrial process systems, HMI can be designed to adapt to the skills and abilities of its

operators to improve fluency in interaction in an extensive system(Villani et al., 2021). The commercial building sector can be embedded with a building automation system for monitoring fan speed and room temperature or in HVAC systems(Hayduk et al., 2016). In addition to its use in the industrial and electricity sectors, HMI-based monitoring has been applied to the transportation sector in truck vehicles capable of self-driving, and touchscreen-based HMI is used to regulate the temperature and window settings of cars (Benderius et al., 2018). The application of HMI in vehicles is to monitor the vehicle cabin's air conditioning system, namely the vehicle's HVAC system. The system has a menu on the HMI, such as setting the temperature mode and monitoring the cabin temperature (Dvorak et al., 2022). In transportation to manage agriculture, an electromyography (EMG) based HMI is used in tractor steering. The device has 14 sensors to measure and process EMG signals from the driver's scalp, and the HMI displays muscle event detection (Gomez-Gil et al., 2011). Apart from various sectors in the field of monitoring applications, especially in the electricity sector, it plays a vital role in detecting anomalies that occur in the electricity network; for example, in the electricity network system, there is an imbalance in voltage and current. The issue is quite significant if it is not monitored how big the imbalance is. One of the studies on the control of two-way converters to inject balanced three-phase current into an imbalanced three-phase system (Vekhande et al., 2016) and also control strategies for micro-grid systems that experience current and voltage imbalances with virtual impedance control (Shi et al., 2016)(Lopatkin & Zinoviev, 2023).

In monitoring three-phase system imbalance using time-frequency-based analysis with superconducting cable media in real-time (Lee et al., 2018). In addition to the power grid system, imbalance monitoring in the application of three-phase induction motors has been proposed with the method of motor current and vibration signals analyzed based on Fast Fourier Transform (FFT), Hilbert Transform (HT), Envelope Detection (ED), and Discrete Wavelet Transform (DWT) to detect the fault level and its possible location under different load conditions (Rahman & Uddin, 2017). Imbalance detection methods with genetic algorithms, namely particle swarm optimization with sigmoid-based acceleration coefficients and chaotic gravitational search algorithm PSOS-CGSA hybrid for status estimation in integrated distribution systems (Ullah et al., 2020), or with probabilistic estimation methods of imbalance in the network by considering daily loading curves load when customarily distributed using the newton Rapson method load flow and simulated with the monte carlo method that can provide a range of voltage imbalance levels for a particular network (Liu & Milanović, 2015), Another way to detect imbalances to protect the power grid in certain areas from such imbalances is to create an algorithm or method where calculating the three-phase voltage and checking the network voltage to the network is lower than the predetermined value of 0.5 pu (per unit) if the value is below the predetermined value then this method immediately gives a trip signal to the system for the protection of the area (Jang & Kim, 2004). In addition to detecting voltage imbalances that occur in the power grid, several new algorithms are proposed for the estimation and diagnosis of current imbalance factors, namely the Circular Phase Shift (CPS) and Circular Cross-Correlation (CCC) algorithms, where data is obtained from multi-sensors and then transmitted and monitored via a remote web server (Hamici & Abu Elhaija, 2019), or the three-phase three-angle algorithm (TP-TA) to detect a Voltage Sag (Madrigal & Rocha, 2007). The result of voltage imbalance can harm drive systems such as three-phase induction motors, namely the occurrence of high vibrations (Campbell & Arce, 2016).

Continuing research has been carried out in the past about the implementation of an energy usage monitoring system in the 3-phase induction motor based on HMI-PowerTag and about the comparison of inrush currents in star, delta, and star-delta types of windings configurations with power quality analyzers and PowerTag (PwT), However, the HMI used is still in the default and cannot display the phase current and phase-neutral voltage imbalance, and cannot display the trend graph of current measurements per phase, as well as the phase-neutral voltage in the three-phase system.

This research aims to design and implement a Human-Machine Interface (HMI) as a tool for monitoring voltage and current imbalances (Tohir et al., 2024)(Tohir et al., 2023). HMI is equipped with a display feature of the percentage of phase-neutral voltage imbalance and phase current in a three-phase system with the Calculation of Maximum Deviation Mean Value

(CMDMV) method based on PowerTag where, in this method, the average value (from current and voltage) is searched for. The maximum deviation value is searched, then from the average value calculated in advance by absoluteizing the value per phase minus the average value, then the largest value of the absolute result is searched, then divided by the average value and converted into a percentage value of imbalance. The results are displayed on the HMI screen. For the detection of current and voltage parameters using the PowerTag module, which module has a current sensor in the form of a current transformer and a voltage sensor, the results of the reading will be sent to the concentrator via wireless, then it will appear in the form of a register which will later be processed in the HMI programming to display the current and voltage imbalance parameters. The expected results of this study HMI can display the percentage of phase current imbalance and phase-neutral voltage. Suppose the percentage of current imbalance is above 5% and the voltage is above 3%. In that case, the display screen indicator value will change to yellow, which means above the threshold value, along with displaying other electrical parameters such as apparent power, active power, reactive power, cos phi, frequency, phase-phase voltage, phase current, neutral current, and current graph trends, voltage and then, the validation form of the results of all these parameters is compared with the power meter and Power Quality Analyzer Meter (PQM) measurements.

3. Research Methods

The method used in this study consists of two stages: the hardware discussion stage of the monitoring simulator and the discussion of the HMI algorithm along with the CMDMV method. The hardware discussion of the simulator includes a switching control circuit for three-phase and single-phase loads that will be borne. The loads to be used are three-phase and single-phase loads with different load properties, ranging from resistive, resistive-inductive, and non-linear load types. For resistive loads in the form of incandescent lamps, for resistive-inductive loads in the form of ballast-based TL lamps, three-phase induction motors, for non-linear loads in the form of semiconductor switching-based equipment, namely, variable speed drives (VSD). For high-power control or switch circuits, components in contactors are used as the primary contacts in disconnecting and connecting electrical power to the load from the power source. The contactor is equipped with a short circuit and overload protection circuit as a three-phase Miniature Circuit Breaker (MCB). Thus, the power circuit for the loads will be well protected if a disturbance occurs. As for the discussion of the HMI algorithm and the CMDMV method, namely by reading the current and voltage parameters using PwT, the data is sent to the concentrator via wireless, then the data from the concentrator will be sent wirelessly to the computer, which then in the HMI algorithm there is to process the electrical parameter registers, then processed in the form of a decimal display of current, voltage, then after that the processed data is entered into the equation to calculate the imbalance with the CMDMV method formulation. The results are displayed as a percentage on the HMI screen with a green indicator, meaning it is by the standard and yellow outside the standard/threshold; then, the results of all these parameters are compared with the power meter and power quality analyzer measurements. The overall system architecture is depicted in Fig.1 below.

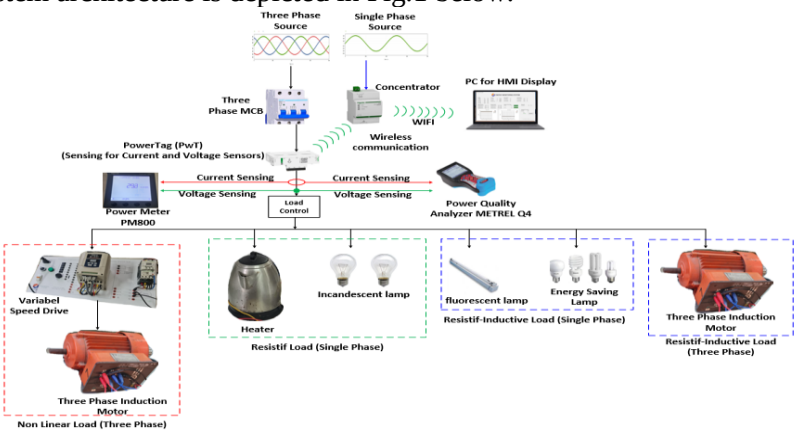

Fig. 1. Overall System Architecture

Fig 1 is the architecture of a simulator system for monitoring current and voltage imbalances in three-phase systems with various loads. The simulator is equipped with overload and short circuit protection and load control in the form of a contactor for breaking and connecting the three-phase source to the load. The load is in the form of TL lamps, incandescent lamps, and heaters, which are 1-phase loads, while three-phase loads are in the form of induction motors controlled by VSD. The active system scheme is when the system is running to perform monitoring, and the PwT will process data in the form of current and voltage sensing that the sensor has carried out. Then, the results of the sensor readings will be sent to the concentrator in the form of a register. Then, each register of electrical measurement parameters will be sent wirelessly, and the data will be processed and calculated digitally, displaying the power per phase, neutral current, energy per phase, and cos phi per phase. The results of these parameters will be displayed on the HMI screen in real-time.

Calculation of Maximum Deviation Mean Value Method

In the Calculation of Maximum Deviation Mean Value (CMDMV) method, the results of the phase current reading and phase-neutral voltage from the sensor are calculated with the initial stage determining the average value of each phase (current and voltage), the second stage determining the maximum deviation value from the average value. The third stage is the result of the second stage, where the highest value is found. Then, it is divided by the value of the results from the second stage and multiplied by one hundred percent. The following is the calculation of the overall percentage of the two parameters (Lee, 1999).

$$IV = \frac{max\left[\left|Van - \frac{Va+Vb+Vc}{3}\right| . \left|Vb - \frac{Va+Vb+Vc}{3}\right| . \left|Vc - \frac{Va+Vb+Vc}{3}\right|\right]}{\frac{Va+Vb+Vc}{3}} x\ 100\% \quad (1)$$

$$IC = \frac{max\left[\left|Ia - \frac{Ia+Ib+Ic}{3}\right| . \left|Ib - \frac{Ia+Ib+Ic}{3}\right| . \left|Ic - \frac{Ia+Ib+Ic}{3}\right|\right]}{\frac{Ia+Ib+Ic}{3}} x\ 100\% \quad (2)$$

Eq. (1) is the percentage of imbalance voltage (IV), while Eq. (2) is the imbalance current (IC). Va, Vb, and Vc are the 3-phase voltages VR-neutral, VS-neutral, and VT-neutral, while Ia, Ib, and Ic are the currents of each phase. For the average value of each phase (current and voltage).

$$V_{avg} = \frac{(Van + Vbn + Vcn)}{3} \quad (3)$$

$$I_{avg} = \frac{(Ia + Ib + Ic)}{3} \quad (4)$$

Eq. (3) and Eq. (4) are the first two stages to determine the average value. For the second stage, follow the following equation.

$$Ia^* = max\left|Ia - \frac{Ia+Ib+Ic}{3}\right| \quad (5)$$

$$Ib^* = max\left|Ib - \frac{Ia+Ib+Ic}{3}\right| \quad (6)$$

$$Ic^* = max \left| Ic - \frac{Ia + Ib + Ic}{3} \right| \quad (7)$$

Eq. (5), Eq. (6), and Eq. (7) for current, as well as for voltage. Then, look for the largest value from the calculation in the three equations and substitute it into the following formula.

$$IC\_total = \frac{Imax^*}{I_{avg}} x100\% \quad (8)$$

From Eq. (8), the $Imax^*$ value is determined by the results of the calculation of Eq.(5), Eq. (6), and Eq. (7), then selected from the results of the calculation which result has the highest value, then the highest value will be entered into the $Imax^*$ variable. Some standards regulate the percentage parameters of imbalance in voltage and current. The voltage imbalance standard refers to IEEE Std 112-2004, which states that the maximum voltage imbalance value is 3%. For current imbalance, according to The American National Standards Institute (ANSI) C84.1-1995, the maximum current imbalance value is 5%. Eq. (1) to Eq. (8) will be entered into the HMI algorithm.

Human Machine Interface Algorithm

Designing Human Machine Interface (HMI) to display electrical parameters such as per-phase current, neutral current, neutral phase voltage, phase-phase voltage, apparent power, active, reactive and power factor, current and voltage imbalance, and current and voltage graph trends, namely, by using visual studio software based on basic language. The initial stage is to design a comprehensive display visualization to provide columns for placing measurement results, then create a data communication system by using a Modbus and a system for retrieving each parameter's address or measurement address stored in the concentrator. Figure 3 is a flowchart of HMI software design displaying electrical parameter values.

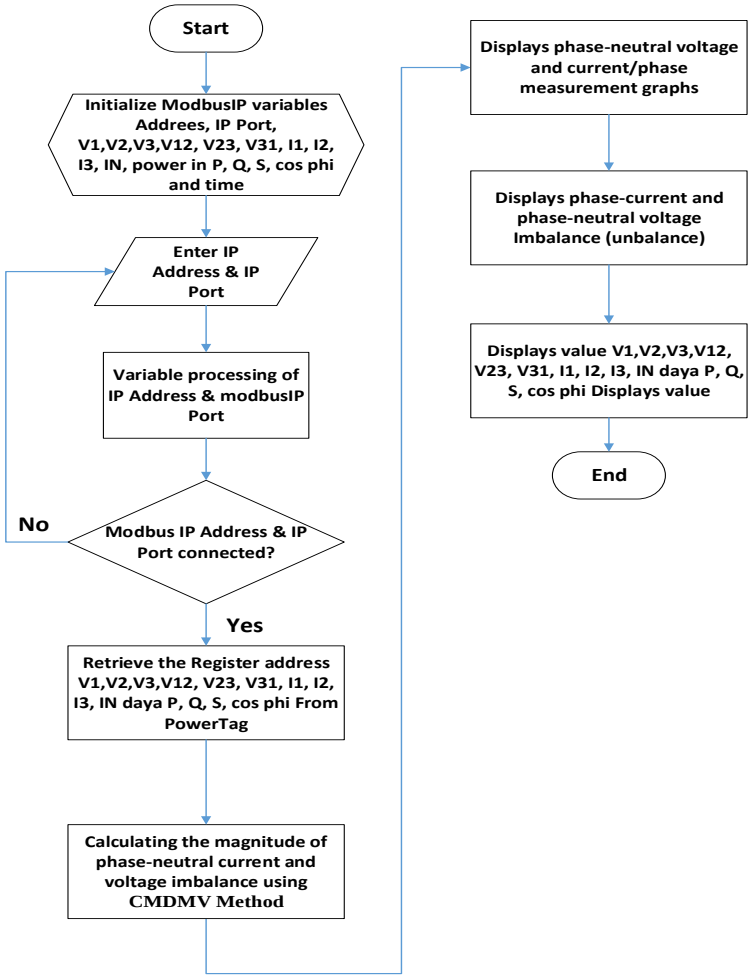

Fig. 2. HMI Software Design Flowchart

Fig. 2 shows a flowchart for designing HMI software using Visual Studio. In the first stage, namely by initializing various variables/parameters such as phase current, neutral current, neutral phase voltage, phase to phase voltage, apparent power, active, reactive, power factor, Modbus IP, IP port used, and monitoring time. Then, a program is designed to read the Modbus IP and IP Port for data communication or retrieval facilities from the concretator to the value display on the HMI. Then, the program will read the IP Port code and Modbus IP. If it does not match, then the program will repeat, but if successful, then the system will take the registered address of each electrical parameter, which will then be processed by the system and can be displayed on the HMI screen.

4. Results and Discussions

This section has two testing stages: balanced and imbalanced loading schemes. It is the result of the software design HMI shown in Fig. 4, which is the implementation stage.

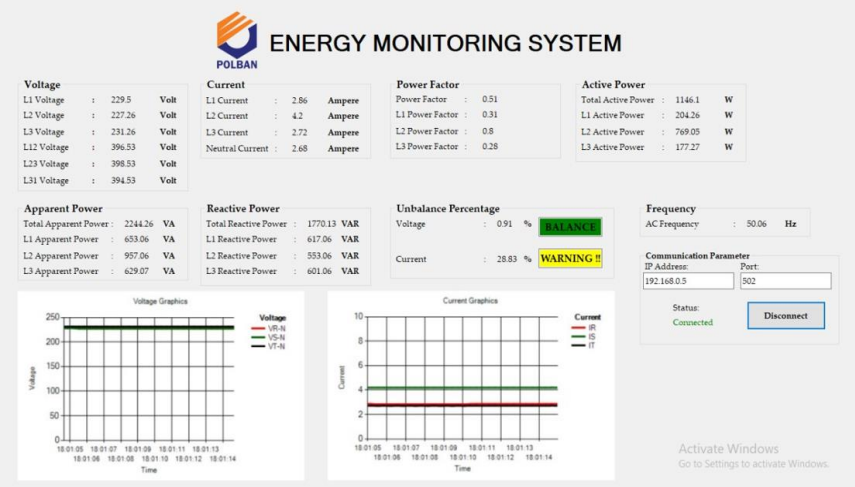

Fig. 3. Results of HMI Display

Fig. 3 above is the result of software implementation. Software is an HMI that can display various electrical parameters such as current and voltage imbalance, power, voltage, phase current, neutral current, cos phi, and frequency. The test scheme is in Fig. 4, while Table 2 contains the following simulator and HMI specifications.

Table 1 - Simulator and HMI Specifications.

Parameter	Information
Type of Current and Voltage Sensors	PowerTag A9MEM1580
Maximum Current	160A
Poles and Wire	3P+4W
Human Machine Interface Programming	Basic Programming
Type of Load	Resistif-Inductive, Resistif and Non-linear Load
Loading Scheme	Unblance and Balance System
Total Phase On Load	Single Phase and Three Phase
Data Connection	Wireless

Table 1 shows the monitoring simulator and HMI software system specifications used. Then, from the loading scheme side, for the current system, the scheme better describes the conditions in the field compared to the previous system. The current parameters measured in the current system are the measurement of phase current and neutral current, which are generally rarely known and often ignored in today's electricity. The reading results listed on the HMI will be compared with the readings of the power meter and power quality analyzer to validate the results of the monitoring system design.

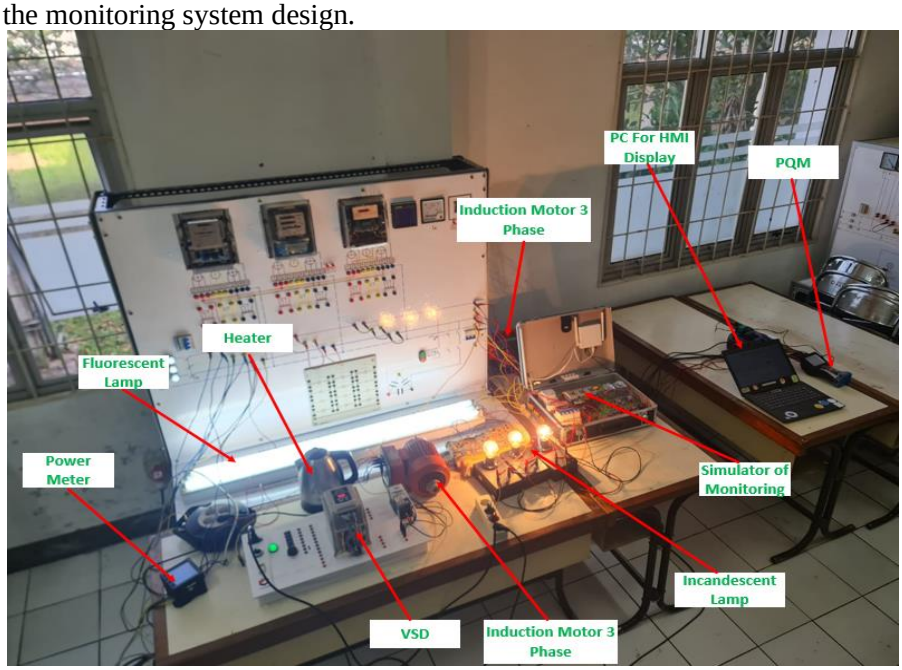

Fig. 4. Overall System Implementation and Testing

Fig. 4 implements the overall system and testing with a balanced and imbalanced 3-phase load scheme by giving each phase a different power load. Ideally, this scheme balances the current, voltage, and electric power. However, when each phase is given an uneven load, it will cause the voltage, current, and power to become imbalanced, and as a result of this imbalance, the appearance of a neutral current. The following is a list of loadings for each phase with an imbalanced scheme.

Table 2 - List of Imbalance Scheme Loads

Phase	Load	Quantity	Power (W)
R	Bulb lamp	1	100
	Fluorescent lamp	1	36
	Induction motor three phase without VSD (No Load)	1	115
S	Bulb lamp	1	100
	Fluorescent lamp	1	36
	Induction motor three phase without VSD (No Load)	1	115
	Induction motor three phase with VSD (No Load)	1	115
	Heater	1	400
T	Bulb lamp	1	100
	Fluorescent lamp	1	36
	Induction motor three phase without VSD (No Load)	1	115

Table 2 lists loading lists with an imbalance scheme on the load side. This scheme tests the designed HMI display's current and voltage imbalance reading. In this scheme, the load that carries the highest power is in the S phase section, which has five different types of loads. Balanced scheme loading reduces the load on the S phase, namely the heater and induction motor, using VSD.

Imbalanced Load Scheme Test Results

In this test, the load carried by the system refers to Table 2, where the load is heterogeneous (single-phase and three-phase loads). In this scheme, we want to see the magnitude of the imbalance on the current side per phase and the phase-neutral voltage. The following image results from the PwT reading displayed on the HMI screen and a power meter to see the imbalance.

(a) (b)

Fig. 5. Imbalance Load Schematic Testing for Current per Phase, (a) HMI, (b) Power Meter

Fig. 5 compares measurements on the Imbalanced load scheme for the current parameters per phase. The test results show that the HMI display screen shows a percentage of current imbalance per phase of 28.83% with a yellow indicator and warning. For measurements using a power meter, the amount of imbalance in the current per phase is 29.2%, with a steady state error reading of 1.26%.

(a) (b)

Fig. 6. Imbalance Load Schematic Testing for Phase-Neutral Voltage, (a)HMI, (b)Power Meter

Fig. 6 is the result of a comparison of measurements on an imbalanced load scheme for the phase-neutral voltage parameter. From the test results, it can be seen that the HMI display screen shows a percentage of phase-neutral voltage imbalance of 0.91% with a green indicator, and according to standards, for measurements using a power meter, the magnitude of the imbalance in voltage is 0.9%, with a steady state error reading of 1.1%. The following graph compares readings between the HMI display screen and the power meter for current and voltage.

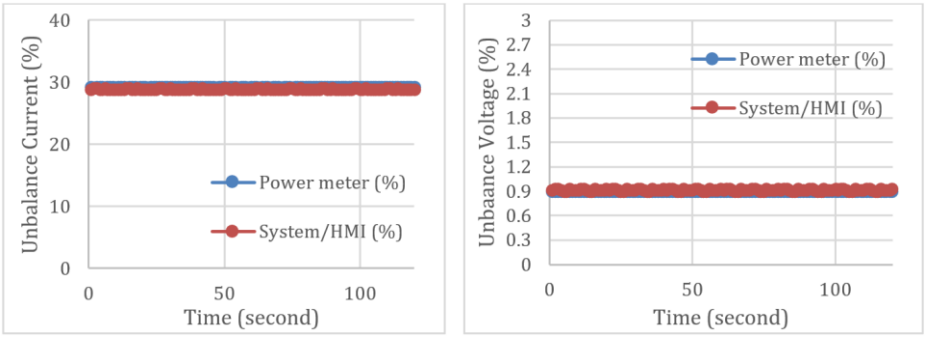

(a) (b)

Fig. 7. Comparison Chart, (a) Current Imbalance Measurement, (b) Voltage Imbalance Measurements

Fig. 7 compares measurements on an imbalanced load scheme for the current parameters per phase between the results of the PwT/system/HMI readings and the power meter readings with a measurement range of 120 seconds or 2 minutes. It can be seen in the graph of Figure 8 that the results of the two measurements overlap each other, indicating that the results of the algorithm that has been designed to read the current imbalance are in good condition. For voltage, compares measurements on an imbalanced load scheme for the phase-neutral voltage parameters between the PwT reading results and the power meter readings with a measurement range of 120 seconds or 2 minutes. It can be seen in the graph of Fig.7 that the results of the two measurements overlap each other, indicating that the results of the algorithm that has been designed to read the voltage imbalance are in good condition. Then, the trend of the current graph per phase from the measurement results using PQM and PwT/HMI System is as follows.

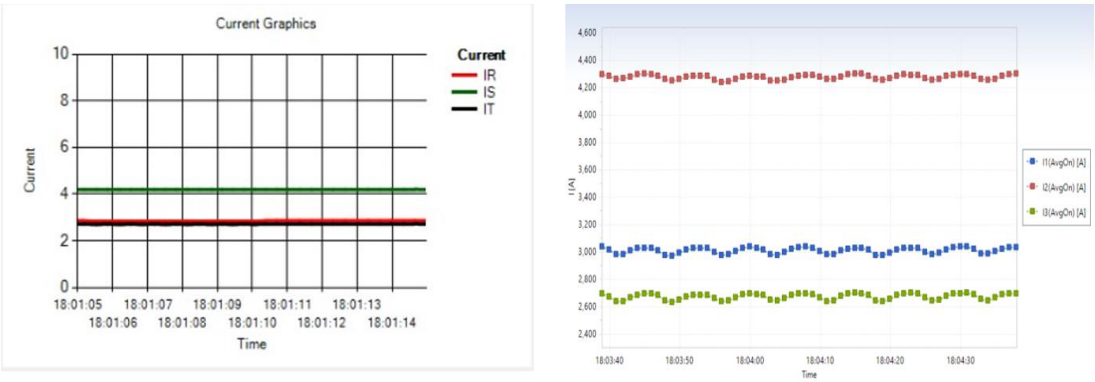

(a) (b)

Fig. 8. Current Profile per Phase Imbalanced Condition, (a) HMI, (b) PQM

Fig. 8 shows the result of the profile of the current per phase in the phase current imbalance scheme between the PQM and HMI monitors. The magnitude of the S phase current is above 4 ampere for both measurements, namely on PQM and PwT.

Balanced Load Scheme Test Results

In this test, the load carried by the system refers to Table 3 by reducing the load in phase S, namely reducing the load of the induction motor equipped with VSD and heater and heterogeneous loads (single-phase and three-phase loads) with a balanced loading scheme. In this scheme, we want to see the imbalance on the current side per phase and the phase-neutral voltage. The following image results from a reading from the system that has been made and a power meter to see the imbalance.

Table 3 - List of Balance Scheme Loads

Phase	Load	Quantity	Power (W)
R	Bulb lamp	1	100
	Fluorescent lamp	1	36
	Induction motor three phase without VSD (No Load)	1	115
S	Bulb lamp	1	100
	Fluorescent lamp	1	36
	Induction motor three phase with VSD (No Load)	1	115
	Heater	1	400
T	Bulb lamp	1	100
	Fluorescent lamp	1	36
	Induction motor three phase without VSD (No Load)	1	115

Table 3 is a list of the loads of each phase with a balanced load scheme. Thus the resulting phase current will be close to balanced as well.

(a) (b)

Fig. 9. Balanced Load Scheme Testing for Current per Phase, (a)HMI, (b)Power Meter

Fig. 9 compares measurements on a balanced load scheme for the current parameters per phase. From the test results, it can be seen that on the HMI display screen, the percentage of current imbalance per phase is 0.96% with a green indicator, and according to the standard, for measurements using a power meter, the magnitude of the imbalance in the current per phase is 1.2%. The current graph trend for each phase on the HMI screen is shown in real-time. The green line is the S phase current, the red line is the current in the R phase, and the black line is for the T phase. It can be seen on the HMI screen that the highest loading is located in the S phase, where, according to Table 8, the R, S, and T phases are schemed to be close to balanced. With this loading scheme, the neutral current side also has a current magnitude close to zero. The phase-neutral voltage parameters are as follows between the readings by the system that has been created and by the power meter.

(a) (b)

Fig. 10. Balanced Schematic Testing for Phase-Neutral Voltage, (a)HMI, (b)Power Meter

Fig. 10 is the result of comparing measurements on a balanced load scheme for phase-neutral voltage parameters. From the test results, it can be seen that the HMI display screen shows a percentage of phase-neutral voltage imbalance of 0.84% with a green indicator. According to standards, for measurements using a power meter, the magnitude of the voltage imbalance is 0.9%. The following graph compares readings between the HMI display screen and the power meter for current and voltage.

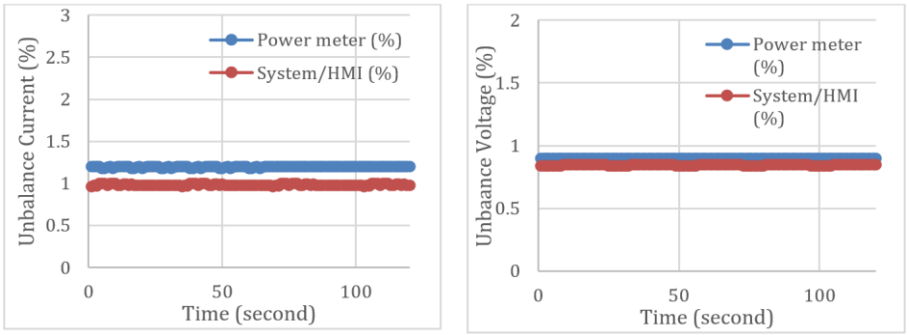

(a) (b)

Fig. 11. Comparison Chart, (a) Current Balance Measurement, (b) Voltage Balance Measurements

Fig. 11 compares measurements on an imbalanced load scheme for phase-neutral voltage and current parameters between the PwT/system/HMI readings and power meter readings with a measurement range of 120 seconds or 2 minutes. It can be seen in the graph of Figure 14 that the results of the two overlapping measurements indicate that the results of the algorithm that has been designed to read voltage imbalances are in good condition. Then, the trend of the current graph per phase from the measurement results using PQM and PwT/HMI System are as follows,

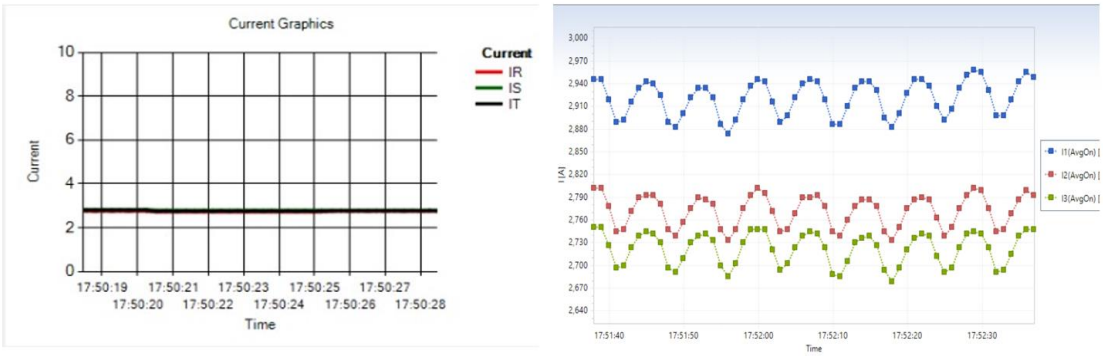

(a) (b)

Fig. 12. Current Profile per Phase Balanced Condition, (a) HMI, (b) PQM

Fig.12 shows the result of the profile of the current per phase in the phase current imbalance scheme between the PQM and HMI monitors. The magnitude of the R, S, and T phase currents is below 3 ampere. For the PQM reading, the R phase is slightly higher than the S and T phases.

5. Conclusion

In the research of the design and implementation of a human-machine interface for monitoring phase current imbalance, phase-neutral voltage with a CMDMV method based on

PowerTag was successfully designed and implemented. A monitoring system with HMI can display power parameters, phase current, neutral current, voltage, and frequency by pulling the register from PowerTag, especially displaying the percentage of current imbalance per phase and phase-neutral voltage. The test results with an imbalanced load scheme stated that the magnitude of the current imbalance reading comparison on the measurement using PowerTag is 28.83% and on the power meter is 29.2% with steady-state error current imbalance reading is 1.27%, while for voltage PowerTag is 0.91% and power meter is 0.9% with steady-state error voltage imbalance reading is 1.11%.

The current and voltage imbalance status indicators can change their color, which is green color when in a balanced condition (BALANCE) and yellow color when the system detects an imbalance in current and voltage (WARNING) in the three-phase electrical network.

Acknowledgement

We want to express our deepest gratitude to the Politeknik Negeri Bandung for providing funding assistance for this research sourced from DIPA with the 2024 Penelitian Madya Utama (PMU) scheme so that the research can be completed properly.

References

Antonijević, M., Sučić, S., & Keserica, H. (2018). Augmented reality applications for substation management by utilizing standards-compliant SCADA communication. *Energies*, *11*(3). https://doi.org/10.3390/en11030599

Basuki, A., Timbar Imam Priadi, Anita Puspita Sari, & Trirohadi, H. (2011). SCADA gateway, smart solution for combining conventional substation and substation automation system. *International Conference on Advanced Power System Automation and Protection*, *2*, 1268–1272. https://doi.org/10.1109/APAP.2011.6180573

Benderius, O., Berger, C., & Malmsten Lundgren, V. (2018). The Best Rated Human-Machine Interface Design for Autonomous Vehicles in the 2016 Grand Cooperative Driving Challenge. *IEEE Transactions on Intelligent Transportation Systems*, *19*(4), 1302–1307. https://doi.org/10.1109/TITS.2017.2749970

Biswal, A., & Bansal, H. O. (2015, February). SCADA and its applications to renewable energy systems integration. *9th International Conference on Industrial and Information Systems*. https://doi.org/10.1109/ICIINFS.2014.7036641

Boakye-Boateng, K., Ghorbani, A. A., & Lashkari, A. H. (2024). Implementation of a Trust-Based Framework for Substation Defense in the Smart Grid. *Smart Cities*, *7*(1), 99–140. https://doi.org/10.3390/smartcities7010005

Bruce, A. G. (1997). Reliability analysis of electric utility SCADA systems. *IEEE Transactions Power Engineering Review*, *17*(12), 59. https://doi.org/10.1109/pica.1997.599397

Campbell, M., & Arce, G. (2016). Effect of motor voltage unbalance on motor vibration: Test and evaluation. *IEEE TRANSACTIONS ON INDUSTRY APPLICATIONS*, *54*(1), 905–911. https://doi.org/10.1109/PCICON.2016.7589243

Castello, P., Ferrero, R., Pegoraro, P. A., & Toscani, S. (2018). Effect of Unbalance on Positive-Sequence Synchrophasor, Frequency, and ROCOF Estimations. *IEEE Transactions on Instrumentation and Measurement*, *67*(5), 1036–1046. https://doi.org/10.1109/TIM.2017.2782013

Craig Wester, Noel Engelman, Terrence Smith, Kehinde Odetunde, Bob Anderson, J. R. (2015). THE ROLE OF THE SCADA RTU IN TODAY'S SUBSTATION. *2015 68th Annual Conference for Protective Relay Engineers*, 622–628.

Czarecki, L. S. (1995). Power related phenomena in three-phase unbalanced systems. *IEEE Transactions on Power Delivery*, *10*(3), 1168–1176. https://doi.org/10.1109/61.400893

Dvorak, D., Krüger, V., & Wang, J. (2022). Innovative HMI and Control Concept for Efficient Thermal Management of Electric Vehicles. *IEEE Transactions on Intelligent Transportation Systems*, *23*(11), 21360–21377. https://doi.org/10.1109/TITS.2022.3177761

Gomez-Gil, J., San-Jose-Gonzalez, I., Nicolas-Alonso, L. F., & Alonso-Garcia, S. (2011). Steering a tractor by means of an EMG-based human-machine interface. *Sensors*, *11*(7),

7110–7126. https://doi.org/10.3390/s110707110

Gu, J. C., Liu, C. H., Chou, K. Y., & Yang, M. T. (2019). Research on CBM of the intelligent substation SCADA system. *Energies*, *12*(20). https://doi.org/10.3390/en12203892

Feola, L., Langella, R., & Testa, A. (2013). On the effects of unbalances, harmonics and interharmonics on pll systems. *IEEE Transactions on Instrumentation and Measurement*, *62*(9), 2399–2409. https://doi.org/10.1109/TIM.2013.2270925

Hamici, Z., & Abu Elhaija, W. (2019). Novel Current Unbalance Estimation and Diagnosis Algorithms for Condition Monitoring with Wireless Sensor Network and Internet of Things Gateway. *IEEE Transactions on Industrial Informatics*, *15*(11), 6080–6090. https://doi.org/10.1109/TII.2019.2935743

Hayduk, G., Kwasnowski, P., & Mikoś, Z. (2016). Building management system architecture for large building automation systems. *Proceedings of the 2016 17th International Carpathian Control Conference*, *June*, 232–235. https://doi.org/10.1109/CarpathianCC.2016.7501100

Jang, S. Il, & Kim, K. H. (2004). An islanding detection method for distributed generations using voltage unbalance and total harmonic distortion of current. *IEEE Transactions on Power Delivery*, *19*(2), 745–752. https://doi.org/10.1109/TPWRD.2003.822964

Kersting, W. H. (2001). Causes and effects of unbalanced voltages serving an induction motor. *IEEE Transactions on Industry Applications*, *37*(1), 165–170. https://doi.org/10.1109/28.903142

Kulkarni, V., Sahoo, S. K., Thanikanti, S. B., Velpula, S., & Rathod, D. I. (2021). Power systems automation, communication, and information technologies for smart grid: A technical aspects review. *TELKOMNIKA (Telecommunication Computing Electronics and Control)*, *19*(3), 1017–1029. https://doi.org/10.12928/TELKOMNIKA.v19i3.16428

Lahti, J. P., Shamsuzzoha, A., & Kankaanpää, T. (2011). Web-based technologies in power plant automation and SCADA systems: A review and evaluation. *2011 IEEE International Conference on Control System, Computing and Engineering, ICCSCE 2011*, 279–284. https://doi.org/10.1109/ICCSCE.2011.6190537

Lee, G. S., Ji, G. H., Kwon, G. Y., Bang, S. S., Lee, Y. H., Sohn, S. H., Park, K., & Shin, Y. J. (2018). Monitoring method for an unbalanced three-phase HTS cable system via time-frequency domain reflectometry. *IEEE Transactions on Applied Superconductivity*, *28*(4). https://doi.org/10.1109/TASC.2018.2809441

Lee, C. Y. (1999). Effects of unbalanced voltage on the operation performance of a three-phase induction motor. *IEEE Transactions on Energy Conversion*, *14*(2), 202–208. https://doi.org/10.1109/60.766984

Liu, Z., & Milanović, J. V. (2015). Probabilistic Estimation of Voltage Unbalance in MV Distribution Networks With Unbalanced Load. *IEEE Transactions on Power Delivery*, *30*(2), 693–703. https://doi.org/10.1109/TPWRD.2014.2322391

Lledó-Ponsati, T., Bahman, A. S., Iannuzzo, F., Montesinos-Miracle, D., & Galceran-Arellano, S. (2021). Effect of current distortion and unbalanced loads on semiconductors reliability. *IEEE access*, *9*, 162660-162670. https://doi.org/10.1109/ACCESS.2021.3133019

Lopatkin, N., & Zinoviev, G. (2023). Overall Currents Unbalance Assessment for Several Three-Phase Loads under Sinusoidal Conditions of Four-Wire Circuit. *Proceedings - 2023 International Ural Conference on Electrical Power Engineering, UralCon*, 160–165. https://doi.org/10.1109/UralCon59258.2023.10291108

Madrigal, M., & Rocha, B. H. (2007). A contribution for characterizing measured three-phase unbalanced voltage sags algorithm. *IEEE Transactions on Power Delivery*, *22*(3), 1885–1890. https://doi.org/10.1109/TPWRD.2007.893438

Mnukwa, S., & Saha, A. K. (2020). SCADA and substation automation systems for the port of durban power supply upgrade. *2020 International SAUPEC/RobMech/PRASA Conference*, 1–5. https://doi.org/10.1109/SAUPEC/RobMech/PRASA48453.2020.9041078

Qasim, I., Anwar, M. W., Azam, F., Tufail, H., Butt, W. H., & Zafar, M. N. (2020). A Model-Driven Mobile HMI Framework (MMHF) for Industrial Control Systems. *IEEE Access*, *8*, 10827–10846. https://doi.org/10.1109/ACCESS.2020.2965259

Rahman, M. M., & Uddin, M. N. (2017). Online Unbalanced Rotor Fault Detection of an IM Drive Based on Both Time and Frequency Domain Analyses. *IEEE Transactions on Industry Applications*, *53*(4), 4087–4096. https://doi.org/10.1109/TIA.2017.2691736

Raman, S. H., Hanafiah, M. A. M., Ab Ghani, M. R., & Jusoh, W. N. S. E. W. (2014). A human machine interface (HMI) framework for Smart Grid system. *2014 IEEE Innovative Smart Grid Technologies - Asia, ISGT ASIA*, 318–322. https://doi.org/10.1109/ISGT-Asia.2014.6873810

Reza, S. M. S., Arifeen, M. M., Tiong, S. K., Akhteruzzaman, M., Amin, N., Shakeri, M., Ayob, A., & Hussain, A. (2020). Salsa20 based lightweight security scheme for smart meter communication in smart grid. *TELKOMNIKA (Telecommunication Computing Electronics and Control)*, *18*(1), 228–233. https://doi.org/10.12928/TELKOMNIKA.V18I1.14798

Silva, M. D., & Ferreira Filho, A. D. L. (2022). An alternative methodology for quantifying voltage unbalance based on the effects of the temperatures and efficiency of induction motors. *IEEE Access, 10*, 83567-83579. https://doi.org/10.1109/ACCESS.2022.3196357

Shi, H., Zhuo, F., Yi, H., & Geng, Z. (2016). Control strategy for microgrid under three-phase unbalance condition. *Journal of Modern Power Systems and Clean Energy*, *4*(1), 94–102. https://doi.org/10.1007/s40565-015-0182-3

Skripcak, T., Tanuska, P., Konrad, U., & Schmeisser, N. (2013). Toward Nonconventional Human–Machine Interfaces for Supervisory Plant Process Monitoring. *IEEE Transactions on Human-Machine Systems*, *43*(5), 437–450. https://doi.org/10.1109/THMS.2013.2279006

Šverko, M., & Grbac, T. G. (2024). Automated HMI design as a custom feature in industrial SCADA systems. *Procedia Computer Science*, *232*(2023), 1789–1798. https://doi.org/10.1016/j.procs.2024.02.001

Tohir, T., Habinuddin, E., Ilman, S. M., & Febi Ariefka, S. P. (2024). Implementation of Energy Usage Monitoring System in 3 Phase Induction Motor Starting. *JTERA (Jurnal Teknologi Rekayasa)*, *9*(1), 21–32. https://doi.org/10.31544/jtera.v9.i1.2024.21-32

Tohir, T., Habinuddin, E., Ilman, S. M., Putra, F. A. S., Anwar, H., & Fadilah, R. (2023). A Comparative Study of Inrush Current on Star, Delta, and Star-Delta Starters for a 1.5kW Three Phase Induction Motor With Power Quality Analyzer and Powertag. *2023 Innovations in Power and Advanced Computing Technologies, i-PACT 2023*, 1–7. https://doi.org/10.1109/I-PACT58649.2023.10434677

Ullah, Z., Elkadeem, M. R., Wang, S., & Radosavljevic, J. (2020). A Novel PSOS-CGSA Method for State Estimation in Unbalanced DG-Integrated Distribution Systems. *IEEE Access*, *8*, 113219–113229. https://doi.org/10.1109/ACCESS.2020.3003521

Vekhande, V., Kanakesh, V. K., & Fernandes, B. G. (2016). Control of Three-Phase Bidirectional Current-Source Converter to Inject Balanced Three-Phase Currents under Unbalanced Grid Voltage Condition. *IEEE Transactions on Power Electronics*, *31*(9), 6719–6737. https://doi.org/10.1109/TPEL.2015.2503352

Villani, V., Sabattini, L., Loch, F., Vogel-Heuser, B., & Fantuzzi, C. (2021). A General Methodology for Adapting Industrial HMIs to Human Operators. *IEEE Transactions on Automation Science and Engineering*, *18*(1), 164–175. https://doi.org/10.1109/TASE.2019.2941541

Vlacic, L., Huang, H., Dotoli, M., Wang, Y., Ioannou, P. A., Fan, L., Wang, X., Carli, R., Lv, C., Li, L., Na, X., Han, Q.-L., & Wang, F.-Y. (2024). Automation 5.0: The Key to Systems Intelligence and Industry 5.0. *IEEE/CAA Journal of Automatica Sinica*, *11*(8), 1723–1727. https://doi.org/10.1109/jas.2024.124635